Resolution of Simultaneous Kinetic Spectrophotometric Process by Factor Analysis

ARTICLE *in* ANALYTICAL CHEMISTRY · MARCH 1993

Impact Factor: 5.64 · DOI: 10.1021/ac00054a010

4 AUTHORS, INCLUDING:

Andreu Cladera Forteza
University of the Balearic Islands
162 PUBLICATIONS **1,242** CITATIONS
SEE PROFILE

Víctor Cerdà
University of the Balearic Islands
1,373 PUBLICATIONS **5,753** CITATIONS
SEE PROFILE

Resolution of Simultaneous Kinetic Spectrophotometric Processes by Factor Analysis

Andreu Cladera, Enrique Gómez, José Manuel Estela, and Víctor Cerdà*

Departament de Química, Universitat de les Iles Balears, E-07071 Palma de Mallorca, Spain

A procedure for the resolution of simultaneous kinetic processes based on the application of factor analysis to a matrix constructed from spectrophotometric data provided by a diode array detector is proposed. The three possible combinations of formation and disappearance kinetic processes involving two analytes are investigated. First, application of principal components analysis to the spectrophotometric data allows the number of simultaneous kinetic processes involved to be determined and hence the spectra and kinetic curves of the individual components to be reconstructed without their prior knowledge. The proposed procedure was satisfactorily applied to kinetic data simulated from Gaussian and real spectra of the Co(II) and Ni(II) complexes of 4-(pyridyl-2-azo)resorcinol (PAR).

INTRODUCTION

Factor analysis is a mathematical method of widespread use in chemical analysis, particularly for resolving overlapped data provided by various techniques.[1,2] Some of its major assets rely on the fact that no standards of the components to be determined or assumption on the shape of their spectra are required.

Ever since Lawton and Sylvester[3] reported the earliest applications of factor analysis for the above purposes there have been a number of significant developments in this context. Thus, gas chromatographic–mass spectrometric data were applied factor analysis in the late 1970s in order to determine the number of components involved in unresolved peaks.[4,5] Later, Chen et al.[6] reconstructed overlapped mass spectra from mixtures of two components by using a modified method based on the Cayley–Hamilton theorem. In this manner, they spared time and computer memory by defining each point in a spectrum from its polar coordinates and the eigenvectors from the covariance matrix. However, it was Sharaf and Kowalski[7,8] who, by using the same analytical technique, accomplished the quantitative resolution of the chromatographic peaks yielded by two coeluted components. By exploiting the increased spectrum acquisition speed of the spectrophotometer used, Osten and Kowalski[9] developed a self-modeling, factor analysis curve resolution method for the resolution of overlapped liquid chromatographic peaks from binary mixtures. The matrix used was constructed from the absorbances measured at six different wavelengths as a function of the elution times of the components. The purest recorded spectra were used as standards. In this way, the overall number of components involved can be determined, binary mixtures resolved, and quantitative results for the two analytes obtained.

Vandeginste et al.[10] took advantage of the potential of diode array spectrophotometric detectors as coupled to HPLC instruments to resolve overlapped peaks involving three rather than two components. They modified the Chen et al. method[6] by assuming that the elution profile of each component was positive, consisted of a single maximum, and that its area—after normalization—was minimal. The method was implemented by previously estimating the purest spectra or the elution profile of each component—this latter choice provided the better results.

More recently, Erickson et al.[11] reported an interesting application of factor analysis to flow injection analysis (FIA) involving the use of a diode array detector for overcoming the interference from background noise. Also, Fay et al. used an HPLC system equipped with an electrochemical detector[12] to investigate the effect of noise on data.[13]

The simultaneous resolution of kinetic processes has so far been addressed by several authors.[14] Thus, by using nonlinear regression methods, Rutan and Brown[15] applied the extended Kalman filter to multiwavelength kinetic data. Also, Pardue et al.[16,17] developed a mathematical model for the kinetic response in the simultaneous determination of catalysts based on differences in the rate of inhibition by a common inhibitor. However, the former methodology requires the prior knowledge of standard spectra, whereas the latter, because of its differential nature, results in dramatically increased errors when the rate constants ratios are close to unity. In addition, both regression models require initial guesses for kinetic and timing parameters, so deviations depend on the estimated values. More recently, Schechter et al.[18] studied kinetic determinations on systems of mixed first- and second-order reactions. They suggested that numerical reconstruction of nonlinear kinetic functions is crucial and should thus be entrusted to the new instrumental techniques, which provide a wealth of kinetic information in an automatic fashion.

In continuation of research into the resolution of multicomponent systems,[19-24] in this work we present a new method

(1) Malinowski, E. R.; Howery, D. *Factor Analysis in Chemistry*; John Wiley & Sons: New York, 1980.
(2) Brown, S. D. *Anal. Chem.* **1990**, *62*, 84R-101R.
(3) Lawton, W. H.; Sylvester, E. A. *Technometrics* **1971**, *13*, 617-633.
(4) Davis, J. E.; Shepard, A.; Stanford, N.; Rogers, L. B. *Anal. Chem.* **1974**, *46*, 821-825.
(5) Malinowski, E. R.; McCue, M. *Anal. Chem.* **1977**, *49*, 284-287.
(6) Chen, J. H.; Hwang, L. P. *Anal. Chim. Acta* **1981**, *133*, 271-281.
(7) Sharaf, M. A.; Kowalski, B. R. *Anal. Chem.* **1981**, *53*, 518-522.
(8) Sharaf, M. A.; Kowalski, B. R. *Anal. Chem.* **1982**, *54*, 1291-1296.
(9) Osten, D. W.; Kowalski, B. R. *Anal. Chem.* **1984**, *56*, 991-995.
(10) Vandeginste, B.; Essers, R.; Bosman, T.; Reijnen, J.; Kateman, G. *Anal. Chem.* **1985**, *57*, 971-985.
(11) Erickson, B. C.; Ruzicka, J.; Kowalski, B. R. *Anal. Chim. Acta* **1989**, *218*, 303-311.
(12) Msimanga, H. Z.; Sturrock, P. E. *Anal. Chem.* **1990**, *62*, 2134-2140.
(13) Fay, M. J.; Proctor, A.; Hoffmann, D. P.; Hercules, D. M. *Anal. Chem.* **1991**, *63*, 1058-1063.
(14) Pardue, H. L. *Anal. Chim. Acta* **1989**, *216*, 69-107.
(15) Rutan, S. C.; Brown, S. D. *Anal. Chim. Acta* **1985**, *167*, 23-27.
(16) Weiser, W. E.; Pardue, H. L. *Anal. Chem.* **1986**, *58*, 2523-27.
(17) Fitzpatrick, C. P.; Pardue, H. L. *Anal. Chem.* **1989**, *61*, 2551-56.
(18) Schechter, I.; Schröder, H. *Anal. Chem.* **1992**, *64*, 325-29.
(19) Gómez, E.; Estela, J. M.; Cerdà, V. *Anal. Chim. Acta* **1991**, *249*, 513-18.
(20) Cladera, A.; Gómez, E.; Estela, J. M.; Cerdà, V. *Int. J. Environ. Anal. Chem.* **1991**, *45*, 143-52.
(21) Gómez, E.; Estela, J. M.; Cerdà, V.; Blanco, M. *Fresenius' J. Anal. Chem.* **1992**, *342*, 318-21.
(22) Cladera, A.; Caro, A.; Gómez, E.; Estela, J. M.; Cerdà, V. *Fresenius' J. Anal. Chem.* **1992**, *342*, 322-26.

0003-2700/93/0365-0707$04.00/0

for the resolution of simultaneous kinetic processes by factor analysis. The potential of this chemometric technique for handling the information provided by kinetic and spectral data is thus exploited to resolve a chemical system without the need to obtain the pure spectra of the analytes involved or the kinetic equations they conform to.

As shown elsewhere,[1,9,10] because of the linear additivity of the signals, the number of components that contribute significantly to the overall absorbance of the process can be determined by applying a principal components analysis of the spectral data. Thus, in order to accomplish better control of the variables to be studied, the proposed method was applied to simulated kinetic processes by using synthetic Gaussian spectra and real spectra for the Co–PAR and Ni–PAR complexes. The formation of the two complexes was simulated by using the kinetic model of Tanaka et al.,[25] where the ligand in the Co(II) and Ni(II) complexes of ethylene glycol bis(2-aminoethyl ether) *N,N,N′,N′*-tetraacetic acid (EGTA) is displaced by PAR according to the following reaction:

$$\text{M–EGTA} + \text{PAR} \rightleftarrows \text{M–PAR} + \text{EGTA}$$

THEORETICAL BACKGROUND

The data to be analyzed are arranged in a matrix **D**, the dimensions of which are NT × NW, where NT is the number of spectra acquired at different times and NW is the number of wavelengths acquired for each spectrum. Each row of **D** corresponds to the spectrum of the mixture at a given point of its kinetics, and each column matches the kinetic curve at a given wavelength.

The first step in determining the number of components that make up the unknown mixture involves calculating the eigenvalues and eigenvectors of the dispersion matrix **D′D** from

$$[\mathbf{D}'\mathbf{D}]\vec{\mathbf{V}}_i = \lambda_i \vec{\mathbf{V}}_i \tag{1}$$

where $\vec{\mathbf{V}}_i$ is the eigenvector i and λ_i its associated eigenvalue. According to the theory of factor analysis, the original matrix **D** can be expressed as a linear combination of the form

$$\mathbf{D} = \mathbf{B}\mathbf{V} + \epsilon \tag{2}$$

where **V** is the factor loading matrix (NC × NW), which is constructed from the first NC eigenvectors of the dispersion matrix, **B** (NT × NC) is the so-called "factor score matrix", and ϵ is an NT × MW matrix that includes errors made in reconstructing the original data matrix. If NC = NW (i.e. if all the eigenvectors are used), then matrix **D** will be fully defined and ϵ will be the zero matrix. However, a few eigenvectors usually contain the whole information on the data structure. The number of such vectors (NC) will be the same as that of compounds with distinct kinetics.

The number of significant eivenvectors is determined by plotting them as a function of the wavelength. The first vector with no significance will also be that resulting in a random distribution (Figure 1). This criterion was found to be better suited to the type of data dealt with in this work than was the percent signficance of the eigenvalues.

Once the number of components involved (NC) has been determined, the factor score matrix is obtained by least-squares regression which, taking into account that the eigenvectors are orthogonal, leads to

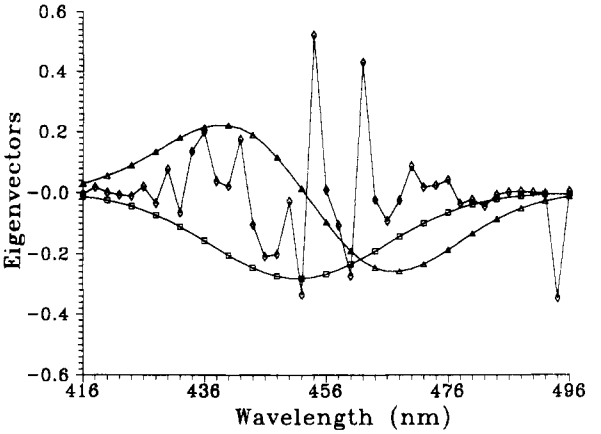

Figure 1. Plot of the first three eigenvectors obtained by processing a matrix of data corresponding to the formation of a product ($k_1 = 4 \times 10^{-3}$ s^{-1}) and the disappearance of a reactant ($k_2 = 4 \times 10^{-3}$ s^{-1}) with Gaussian spectra (M_1 = 450 nm, M_2 = 457 nm, $s_1 = s_2$ = 14 nm): (□) first eigenvector; (△) second eigenvector (◇); third eigenvector.

$$\mathbf{B} = \mathbf{D}\mathbf{V}' \tag{3}$$

Thus, for a two-component system, any acquired spectrum can be reconstructed by using the following equation:

$$\vec{\mathbf{M}}_i = b_{i,1}\vec{\mathbf{V}}_1 + b_{i,2}\vec{\mathbf{V}}_2 \tag{4}$$

where $\vec{\mathbf{M}}_i$ is the ith acquired spectrum, and $b_{i,1}$ and $b_{i,2}$ are the corresponding factor scores as calculated from eq 3. By normalizing all the $\vec{\mathbf{M}}_i$ and $\vec{\mathbf{B}}_i$ vectors according to

$$\hat{m}_{ij} = \frac{m_{ij}}{\|\vec{\mathbf{M}}_i\|} \; \forall j = 1, 2, ..., \text{NW} \tag{5}$$

$$\hat{b}_{i,l} = \frac{b_{i,l}}{\|\vec{\mathbf{B}}_i\|} \; l = 1, 2$$

$\vec{\mathbf{B}}_i$ can be expressed in polar coordinates, so eq 4 can be transformed into

$$\hat{\mathbf{M}}_i = \cos\phi_i\vec{\mathbf{V}}_1 + \sin\phi_i\vec{\mathbf{V}}_2 \tag{6}$$

$$\phi_i = \arcsin(\hat{b}_{i,2})$$

Thus, each spectrum of the working set will be defined by ϕ, and the spectra of the two pure components by

$$\hat{S}_{\text{I}} = \cos\phi_{\text{I}}\vec{\mathbf{V}}_1 + \sin\phi_{\text{I}}\vec{\mathbf{V}}_2 \tag{7}$$

$$\hat{S}_{\text{II}} = \cos\phi_{\text{II}}\vec{\mathbf{V}}_1 + \sin\phi_{\text{II}}\vec{\mathbf{V}}_2$$

Therefore, obtaining the spectra of the two pure components is reduced to determining the angles ϕ_{I} and ϕ_{II}.

Osten et al.[8] and Vandeginste et al.[9] recommend using two constraints in determining pure spectra from high-performance liquid chromatographic (HPLC) data, namely: (a) the pure spectra cannot hold negative absorbance values and (b) all the spectra of the working set can be expressed as a linear combination of the pure spectra, the coefficients of which must be positive. The latter constraint can be expressed mathematically as follows:

$$\hat{M}_i = \alpha_i\hat{S}_{\text{I}} + \beta_i\hat{S}_{\text{II}} \tag{8}$$

$$\alpha_i \geq 0 \qquad \beta_i \geq 0$$

Application of the two constraints yields a set of solutions for each pure spectrum of the form

(23) Cladera, A.; Caro, A.; Gómez, E.; Estela, J. M.; Cerdá, V. *Talanta* **1992**, *39*, 887–91.
(24) Turnes, G.; Cladera, A.; Gómez, E.; Estela, J. M.; Cerdà, V. *J. Electroanal. Chem. Interfacial Electrochem.* **1992**, *338*, 49–60.
(25) Tanaka, M.; Funahashi, S.; Shirai, K. *Anal. Chim. Acta* **1967**, *39*, 437–445.

$$\phi_I^i \le \phi_I \le \phi_I^\circ \qquad (9)$$

$$\phi_{II}^\circ \le \phi_{II} \le \phi_{II}^i$$

where the inner bounds (ϕ_I^i, ϕ_{II}^i) are defined by the second constraint and correspond to the purest recorded spectra

$$\phi_I^i = \max(\phi_i) \qquad (10)$$

$$\phi_{II}^i = \min(\phi_i)$$

Any spectrum such that $\phi_I^i > \phi > \phi_{II}^i$ can be expressed as a combination of these bounds and will therefore be less pure. The outer bounds are defined by the first constraint and are of the following form:

$$\phi_I^\circ = \arcsin\left(\min_{v_{2i}<0}\sqrt{\frac{v_{1,j}^2}{v_{1,j}^2 + v_{2,j}^2}}\right) \qquad (11)$$

$$\phi_{II}^\circ = \arcsin\left(-\min_{v_{2i}\ge 0}\sqrt{\frac{v_{1,j}^2}{v_{1,j}^2 + v_{2,j}^2}}\right)$$

where $v_{1,j}$ and $v_{2,j}$ are the j components of the first two eigenvectors and provide the ϕ values at which one of the absorbances is zero.

Let us consider two cases of special interest. In one of them, the spectra corresponding to the pure components are obtained at some stage in the data acquisition process, which is commonplace in chromatography when two peaks are not fully overlapped. In this situation, the inner bounds (ϕ_I^i, ϕ_{II}^i) coincide with the spectra of the pure components. In the second special case, the pure compounds possess characteristic wavelengths (i.e. each compound absorbs at a given wavelength where the other does not). In this case, the spectra of the pure components coincide with the outer bounds (ϕ_I°, ϕ_{II}°). If both situations concur, then the inner and outer bounds coincide and the pure spectra are exactly defined. On the other hand, if neither situation occurs, then the solution band broadens—the farther the actual situation is from these two, the broader will be the bands—and the real solution will lie at an intermediate point in the range that cannot be determined without supplementary information.

Once ϕ_I and ϕ_{II} have been determined, the corresponding normalized pure spectra can be obtained from eq 7. On the other hand, by combining eqs 6 and 8 one has

$$\alpha_i = \frac{\sin\phi_i - \tan\phi_{II}\cos\phi_i}{\sin\phi_I - \tan\phi_{II}\cos\phi_I} \qquad (12)$$

$$\beta_i = \frac{\sin\phi_i - \tan\phi_I\cos\phi_i}{\sin\phi_I - \tan\phi_I\cos\phi_{II}}$$

where α_i and β_i are the contributions of each pure compound to the ith acquired spectrum. Finally, the individual curve of each compound can be readily obtained by eliminating the normalization introduced into eq 5 as follows

$$\tilde{\mathbf{M}}_i^I = \alpha_i \hat{\mathbf{S}}_I \|\tilde{\mathbf{M}}_i\| \qquad (13)$$

$$\tilde{\mathbf{M}}_i^{II} = \beta_i \hat{\mathbf{S}}_{II} \|\tilde{\mathbf{M}}_i\|$$

where $\tilde{\mathbf{M}}_i^I$ and $\tilde{\mathbf{M}}_i^{II}$ are the spectra of the two components at point i.

EXPERIMENTAL SECTION

Kinetic data are simulated and processed by means of the program FASIMKIN developed by the authors. (The software used can be obtained on request from SCIWARE, Banco de Programas, Departamento de Química, Universitat de les Illes Balears, E-07071 Palma de mallorca, Spain.) First, it generates a matrix of absorbance data subjected to a preset amount of experimental noise as a function of the time and wavelength corresponding to the time course of two or more compounds that follow an increasing (or decreasing) first-order kinetics. The

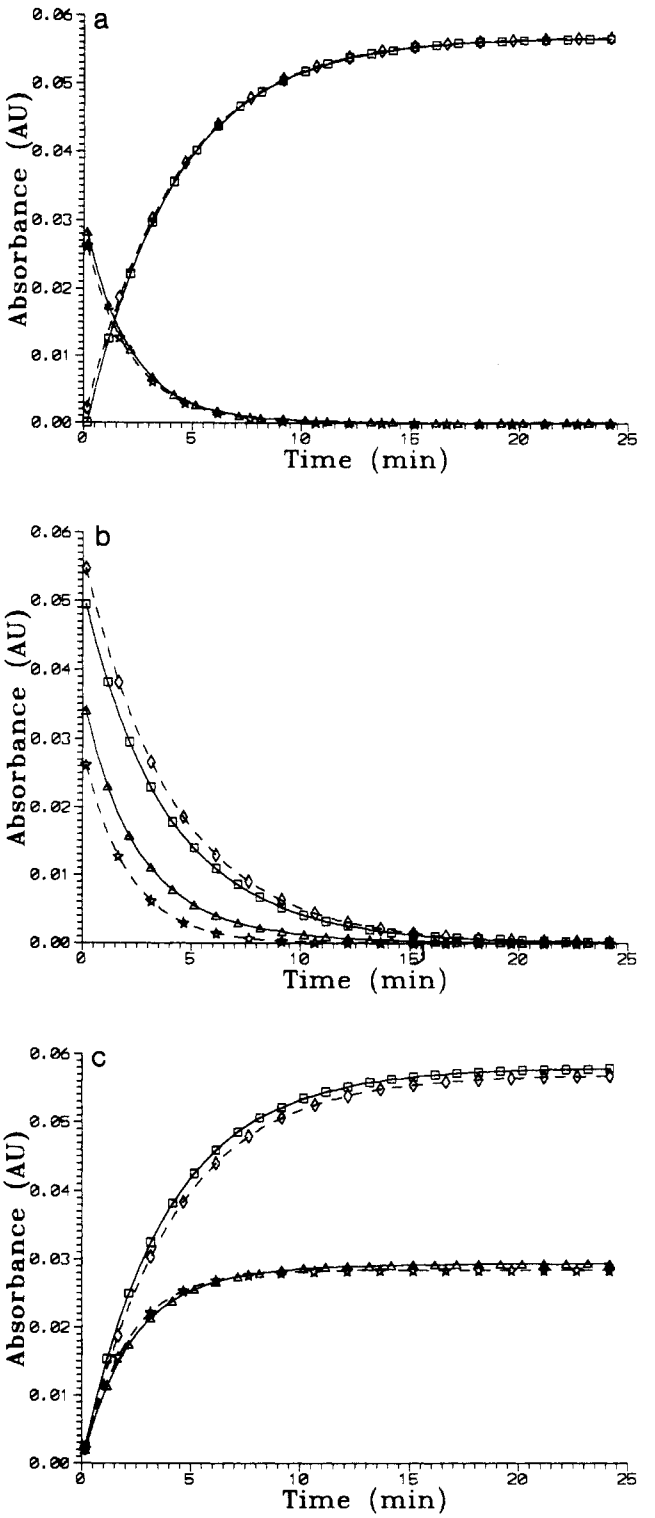

Figure 2. Simulated and reconstructed kinetic curves corresponding to (a) formation of a product (component 1) and disappearance of a reactant (component 2); (b) disappearance of two reactants; and (c) formation of two products. Conditions: $k_1 = 0.004\ s^{-1}$, $k_2 = 0.08\ s^{-1}$, $C_1/C_2 = 2.0$, $\sigma = 0.5$, imprecision = 0.001, delay time = 10 s, overall time = 25 min, interval between readings = 30 s, wavelength range = 410–496 nm, wavelength interval = 2 nm; (□) component 1, simulated; (◇) component 1, reconstructed; (△) component 2, simulated; (☆) component 2, reconstructed.

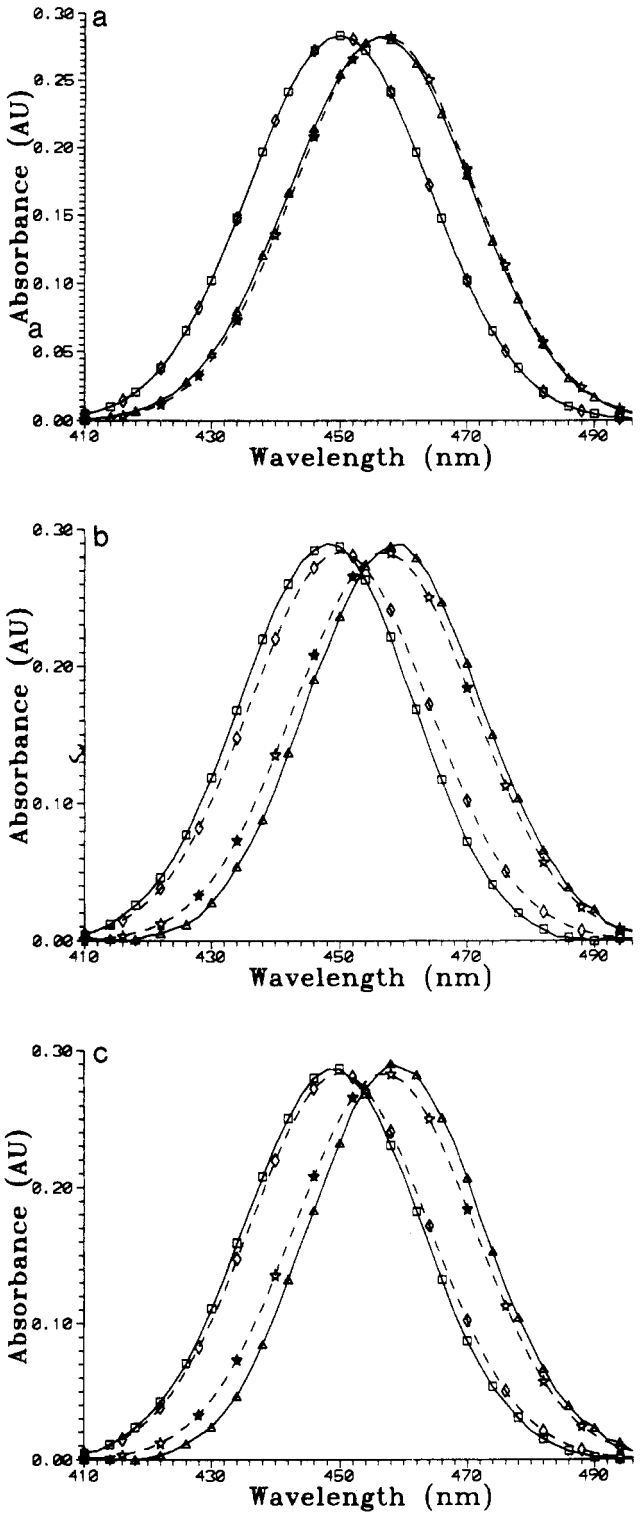

Figure 3. Simulated and reconstructed spectra corresponding to the three kinetic processes illustrated in Figure 2: (□) component 1, simulated; (◇) component 1, reconstructed; (△) component 2, simulated; (☆) component 2, reconstructed.

spectra of the compounds concerned can either be obtained by using a Gauss function or be real experimental spectra. We used synthetic data matrices throughout because they allow better monitoring of the different variables affecting kinetic processes. In order to simulate a real situation as closely as possible, we subjected all data to lag phase of 10 s between the start of data acquisition and that of the kinetics itself. This interval, together with the rates of the kinetics concerned, determines whether or not obtaining a virtually pure spectrum of each reactant is possible. The overall time used to monitor kinetic processes was 25 min.

Previously generated data are processed to calculate the eigenvectors and eigenvalues of the corresponding covariance matrix. Then, the program performs all other calculations required to reconstruct the spectra of the pure components and the individual kinetic curves. Finally, the program provides the corresponding errors. The input concentrations and constant rates are obtained by using a linear regression method.

The spectra of the Co–PAR and Ni–PAR complexes referred in the Applicability section below were obtained from solutions containing 1 μg/mL of either metal and 2×10^{-4} M 4-(pyridyl-2-azo)resorcinol (PAR) in a 0.02 M borate/boric buffer of pH 8.5 to which EGTA was subsequently added up to a 10^{-3} M concentration in order that equilibrium be rapidly reached. Spectra were recorded against a reagent blank by using a Hewlett-Packard HP 8452A diode array spectrophotometer.

RESULTS AND DISCUSSION

The kinetic evolution of a mixture of two components can be studied by monitoring the appearance of the reaction products, the disappearance of the reactants, or the appearance of one product and disappearance of one reactant. Each of these alternatives requires a different approach to the reconstruction of the individual processes and is dealt with in detail below for first-order kinetics.

Monitoring of the Appearance of a Reaction Product and Disappearance of a Reactant (Type I). At time zero, the reactant will exhibit its maximum absorbance, whereas the product will show no absorbance as none of it will have been formed. After some time, though, the reactant will have virtually disappeared, whereas the product will be present at its maximum concentration. Accordingly, a spectrum recorded at time zero will be representative of the pure reactant, whereas that of the pure product will only be recorded after it has reached its maximum absorbance. Therefore, taking into account the above theoretical considerations, the pure spectra of the two compounds can be obtained from the inner bounds of the solution band for angle ϕ.

Monitoring of the Disappearance of the Two Reactants (Type II). In this case, the pure spectrum of either component after time zero will not be available until the faster-reacting component has disappeared completely. Only after that will one be able to obtain the spectrum of the slower-reacting component. Consequently, the most appropriate criterion for selecting angle ϕ will be that of the inner bound for the slower reaction and that of the outer bound for the faster reaction. In any case, one should bear in mind that, because of the very nature of this type of process, even if a virtually pure spectrum of the slower-reacting compound can be obtained by the end of the kinetics, the sensitivity of the determination will be lower owing to the low absorbances to be expected for this region. On the other hand, if the spectrum of the faster-reacting component envelops the whole spectrum of its slower counterpart, the former will be unresolvable. In such a case, the angle ϕ corresponding to the real spectrum of the former will lie at an intermediate point within the solution band that can only be determined with the aid of additional information (e.g. the shape of the individual spectrum).

Monitoring of the Appearance of the Two Reaction Products (Type III). In the third case, neither pure spectrum can be obtained owing to the nature of the kinetic process. Therefore, the criterion to be used in selecting angle ϕ for the two components will be that of the outer bounds of their respective solution bands. As stated above, resolving this type of kinetics is possible provided the two spectra are not fully overlapped (i.e. as long as one is not fully enveloped by the other). As in the previous section, if this is the case, the resolution can only be accomplished if additional information on the enveloping spectrum is available.

Table I. Experimental Conditions Used To Study Different Variables in the Resolution of Simultaneous Kinetics of Formation of a Product (Component 1) and Disappearance of a Reactant (Component 2), Disappearance of Two Reactants, and Formation of Two Products[a]

figure	x-axis variable	y-axis variable	variation ranges X	variation ranges Y	constants
4	wavelength range	imprecision	1–4 nm	0–0.01	λ range = 400–506 nm
5	imprecision	time interval	0–0.01	30–120 s	λ range = 400–506 nm
6	spectral overlap	wavelength range	0.1–1.0	16–206 nm	time interval = 60 s
7a	spectral overlap	k_1/k_2	0.1–1.0	0.2–5.0	λ range = 410–496 nm, time interval = 60 s
7b,c	spectral overlap	k_1/k_2	0.1–1.0	0.2–0.9	λ range = 410–496 nm, time interval = 30 s

[a] The following parameters were kept constant at the stated values except when used as variables or if otherwise stated on the Constants column. $k_1 = 0.004\ s^{-1}$; $k_2 = 0.008\ s^{-1}$; $\sigma = 0.5$; imprecision = 0.001; wavelength interval = 2 nm; delay time between the beginning of kinetics and that of data acquisition = 10 s; overall kinetics monitoring time = 25 min; spectral maxima, M_1 = 450 nm and M_2 = 457 nm; width at half height = 14 nm; identical concentrations of the two components.

Figure 2 shows typical simulated and reconstructed kinetic curves for the three monitoring procedures. They reflect the typically good resolution achieved when the pure spectra of both components are available. Figure 3 shows the spectra corresponding to these experiments.

Factors Influencing the Reconstruction of Individual Kinetic Processes. Table I summarizes the experimental conditions for the most significant simulations and lists the investigated variables, studied ranges, and parameters that were kept constant in each case. For technical reasons, only two variables were changed, all others being kept at reasonable values in each group of simulations in order to isolate problems.

Imprecision and Size of the Data Matrix. We first studied the implications of imprecision in the data of the generated matrix and the number of points it contained on the resolution by using each of the three models for simultaneous kinetic processes. Noise was introduced at each point by a random process involving calculation of the average of ten randomly obtained numbers between −1 and +1 in order to achieve a roughly normal noise distribution and multiplying the result by the corresponding imprecision. Figure 4 shows the mean errors made in reconstructing the two individual kinetic processes as a function of imprecision and the number of wavelengths used in the three types of reconstruction. As in the following sections, errors were calculated as the means of the values obtained for each of the two kinetics by using the equation

$$\text{error (\%)} = \frac{\sqrt{\sum_{t=1}^{NT}(A_{theo} - A_{calc})^2}}{\sum_{t=1}^{NT} A_{theo}} \times 100$$

where A_{theo} and A_{calc} are the theoretical and calculated absorbances at each wavelength of maximum absorption, respectively.

The imprecision in the absorbance signal values ranged from 0 to 0.01. The points corresponding to the wavelengths were processed over the range 400–506 nm at intervals between 1 and 4 nm, which entailed using NT × NW matrices of sizes from 26 × 107 to 26 × 28 points.

As one would expect from the nature of the mathematical procedure used, errors increased with increasing imprecision and decreasing matrix size. However, while the mean errors for type I kinetics were fairly small (less than 5%) in all experiments, the other two kinetic models required imprecisions smaller than 0.002 and wavelength intervals not wider than 2 nm for acceptable errors to be obtained. The results also reveal that, while the errors made in the reconstruction of the two individual type III kinetics are of the same order, those of the type I and type II kinetics are smaller in that with the smaller rate constant.

On the other hand, on evaluating the number of points in relation to the time intervals elapsed between two successive readings, we found that, as with NW, errors increased with increasing imprecision and decreasing number of points in the matrix. Thus, by using wavelength intervals of 2 nm we studied time intervals between 30 and 120 s, which provided NT × NW sizes from 51 × 54 to 13 × 54 points. As can be seen in Figure 5, while errors in type I kinetics were always relatively small, type II and type III kinetics called for imprecisions less than 0.002 and time intervals shorter than 30 s for acceptable errors to be obtained.

According to the above results, one may assume that the number of replicates to be used in each experiment will essentially depend on the model employed and the imprecision in the readings. Thus, while type I kinetics can be processed in a single experiment thanks to the small deviations involved, type II and type III kinetics should be repeated a number of times. By way of example, if one uses 26 × 54 matrices and an imprecision of 0.001 with simultaneous formation kinetics, then the mean error obtained from three replicates is 1.93% and the standard deviation was ±0.29. However, if the imprecision is doubled, then the number of replicates required to obtain errors of the same order (2.39%) is 10, even though the standard deviation increases considerably (to ±1.38).

Degree of Spectral Overlap and Wavelength Range Amplitude. From the above results we chose an imprecision of 0.001 and a matrix size corresponding to time and wavelength intervals of 30 s and 2 nm, respectively, for subsequent experiments. The degree of spectral overlap (σ) is expressed as the relationship between the distance between maxima of the two absorption bands and their width at half height. The studied values ranged between 0.1 and 1.0 since, because of the very foundation of the procedure, a zero σ value would not allow the two simultaneous kinetic processes to be resolved.

Likewise, in order to determine the effect of the amplitude of the wavelength range over which the mathematical treatment was applied, we centered it at 453 nm in every case. The amplitudes assayed ranged from 16 to 206 nm. Figure 6 illustrates the behavior of the three kinetic models as a function of these two variables. As can be seen and one would expect, errors increased with increasing degree of overlap (decreasing σ), as well as for too wide or narrow wavelength ranges. This can be ascribed to a given wavelength range that exceeds the limits of the two absorption bands not contributing significantly in such a way that the errors made in reconstructing the kinetics may rise considerably as a result of the virtually nil absorbance values involved. On the other hand, rather narrow working ranges will logically result in the loss of excessive information and hence in substantially increased errors.

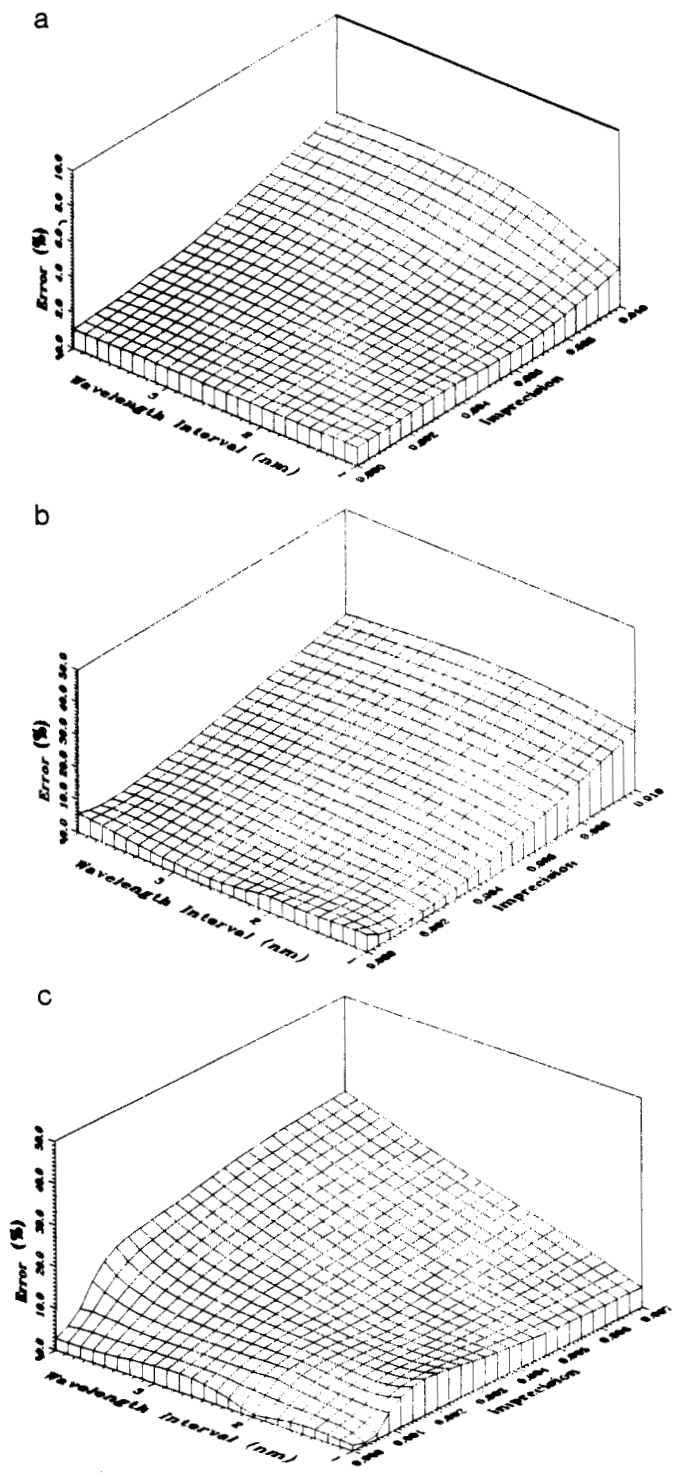

Figure 4. Percent errors obtained in studying the wavelength range used as a function of the imprecision: (a) formation of a product (component 1) and disappearance of a reactant (component 2); (b) disappearance of two reactants; and (c) formation of two products. Working conditions as in Table I.

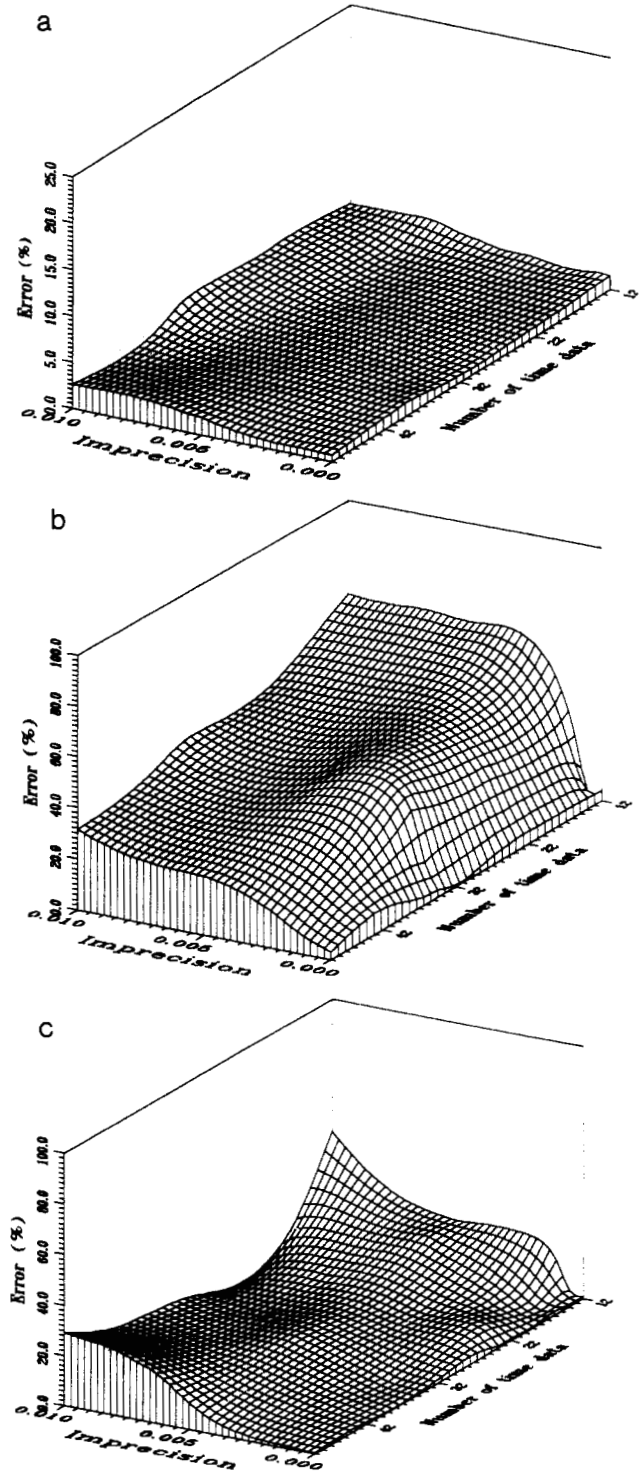

Figure 5. Percent errors obtained in studying the imprecision as a function of the interval between successive readings: (a) formation of a product (component 1) and disappearance of a reactant (component 2); (b) disappearance of two reactants; and (c) formation of two products. Working conditions as in Table I.

Rate Constant Ratios. Once the values of the variables described in the previous sections were fixed (imprecision = 0.001, wavelength interval = 2 nm, interval between readings = 30 s, and working wavelength rage = 410–496 nm), we investigated the effect of the ratio between the rate constants of the kinetic processes as a function of spectral overlap. Figure 7 shows the errors obtained by using each of the three kinetic models as a function of these two variables. While the variation range of spectral overlap was always the same as in Figure 6, the rate constant ratios depended on the model used. Thus, type I kinetics, which involves two reactions of opposing evolution, was studied at rate constant ratios between 0.2 and 5.0. On the other hand, type II and type III kinetics, which involve reactions evolving in the same direction, were studied at ratios between 0.2 and 0.9. As can be seen in Figure 7a, the kinetic model used was only slightly affected by either variable and the errors were always less than 2%. However, the errors for type II and type III kinetics (Figure 7b,c) increased as the two rate constants approached each other. Even so, such errors were acceptable in most cases; thus, for $\sigma = 0.5$ and a rather unfavorable ratio, $k_1/k_2 = 0.9$, the mean error made in reconstructing the two

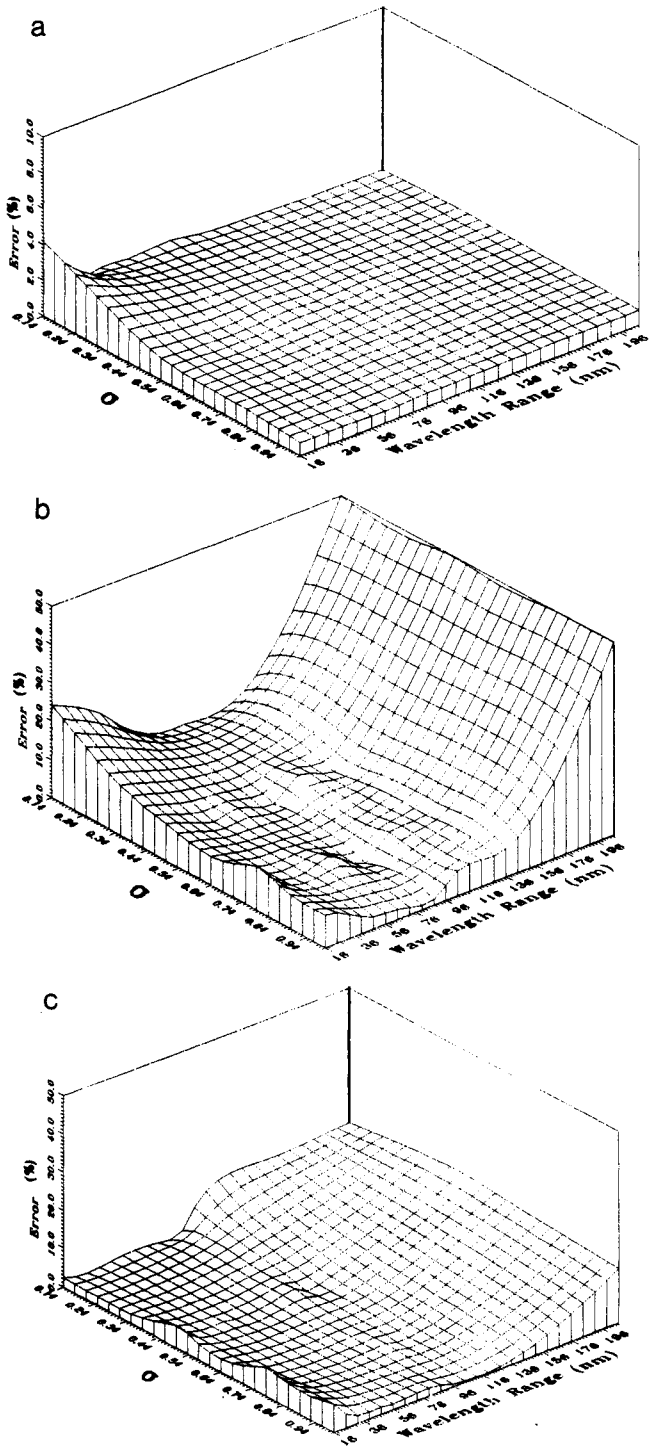

Figure 6. Percent errors obtained in studying the degree of overlap as a function of the amplitude of the wavelength range used: (a) formation of a product (component 1) and disappearance of a reactant (component 2); (b) disappearance of two reactants; and (c) formation of two products. Working conditions as in Table I.

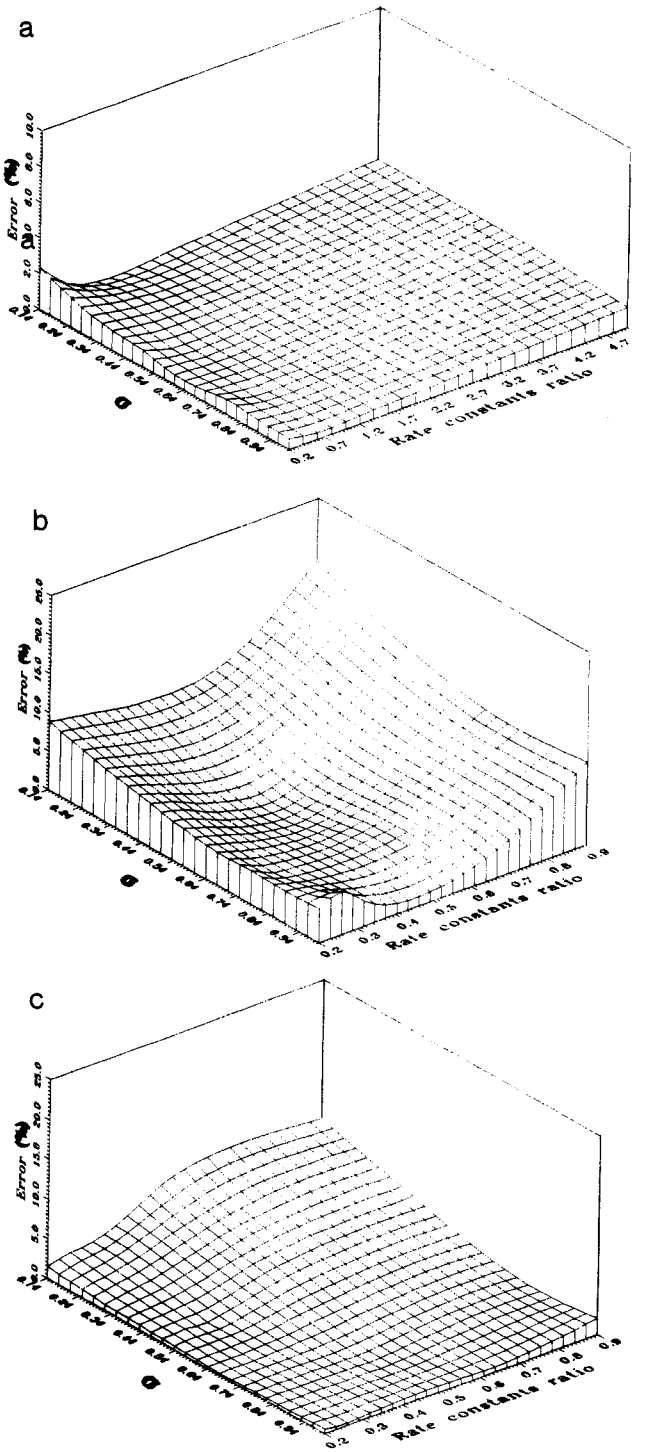

Figure 7. Percent errors obtained in studying the degree of overlap as a function of the rate constant ratio used: (a) formation of a product (component 1) and disappearance of a reactant (component 2); (b) disappearance of two reactants; and (c) formation of two products. Working conditions as in Table I.

simultaneous kinetic processes was 11.8% (disappearance) and 3.8% (formation), respectively.

From the results obtained in the above-described experiments it follows that in type II processes, improvements in the values of the experimental variables benefit the slower reacting component to a greater extent, whereas in type III processes both kinetics are similarly affected.

On the other hand, in models I and II, the overall monitoring time to be used will be determined by that required for the corresponding component to disappear completely if the spectrum of the other, pure component is to be recorded. If such a time is rather too long, one can always resort to the procedure involved in model III, which uses the outer bounds of the respective solution bands for angle ϕ.

Once the effect of the different experimental variables on the reconstruction of the individual kinetics was investigated, we analyzed the implications of using different concentration ratios of the two components, which in principle, should reflect the degree of overlap and the rate constant values. Table II lists the recoveries obtained at different concentration ratios by using the three kinetic models. The results obtained were satisfactory as a whole, with the exception of type II processes

Table II. Recoveries of the Two Components Obtained at Different Concentration Ratios for Simultaneous Formation–Disappearance (Type I), Disappearance–Disappearance (Type II), and Formation–Formation (Type III) Kinetics

C_1/C_2	type I[a]	type II	type III
10.0	103–137	100–106	86–200
5.0	104–120	97–119	88–170
2.0	104–107	90–122	92–116
1.0	103–104	99–109	101–100
0.5	103–102	111–95	100–101
0.2	103–101	105–100	175–88
0.1	103–100	168–95	200–86

[a] Component 1 was formed and component 2 disappeared in type I kinetics. The working conditions used were as follows: $k_1 = 0.004$ s^{-1}; $k_2 = 0.008$ s^{-1}; $\sigma = 0.5$; imprecision = 0.001; wavelength interval = 2 nm; delay time between the beginning of kinetics and that of data acquisition = 10 s; time interval = 30 s; overall kinetics monitoring time = 25 min; spectral maxima, $M_1 = 450$ nm and $M_2 = 457$ nm; width at half height = 14 nm.

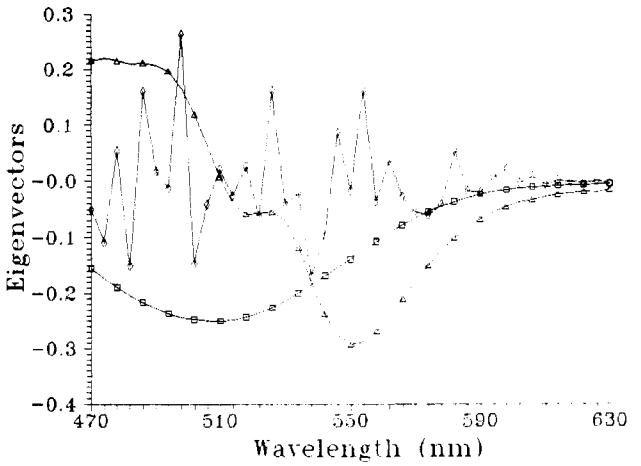

Figure 8. Plot of the first three eigenvectors obtained by processing a data matrix corresponding to the formation of two products ($k_1 = 10^{-3}$ s^{-1}, $C_1 = 1$ mg/L, $k_2 = 5 \times 10^{-5}$ s^{-1}, $C_2 = 1$ mg/L), the spectra of which correspond to the Co–PAR (component 1) and Ni–PAR complexes (component 2): (□) first eigenvector; (△) second eigenvector; (◇) third eigenvector.

in those cases where the slower disappearing component was present at a much lower concentration than the other, as well as in type III processes whenever either component was much less concentrated than the other.

Applicability. By way of example, let us consider the formation of the Co–PAR and Ni–PAR complexes by displacement from their respective EGTA complexes and assumed the kinetics involved to be first-order.

First, we obtained the real spectra of the two complexes as described in the Experimental Section. The spectrum of the Ni–PAR complex was enveloped by that of the Co–PAR complex, so this was the most unfavorable case of those discussed above and called for additional information if appropriate resolution was to be accomplished. These spectra were used to simulate the evolution of the kinetics concerned by means of the program FASIMKIN.

As can be seen in Figure 8, only two of the eigenvectors obtained from the data matrix provided significant information. Figure 9 shows the solution bands obtained for Co–PAR and Ni–PAR on the basis of their reconstructed spectra. As shown above, the Ni–PAR spectrum could be determined from the outer bound of the corresponding solution band. On the other hand, the real spectrum of Co–PAR lies in an intermediate zone of its solution band. Taking into account that the spectrum of the Co–PAR complex was known (as in the determination of Co in the presence of a unknown

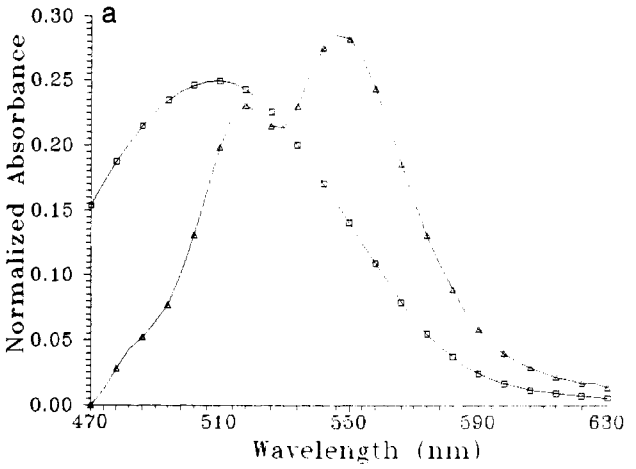

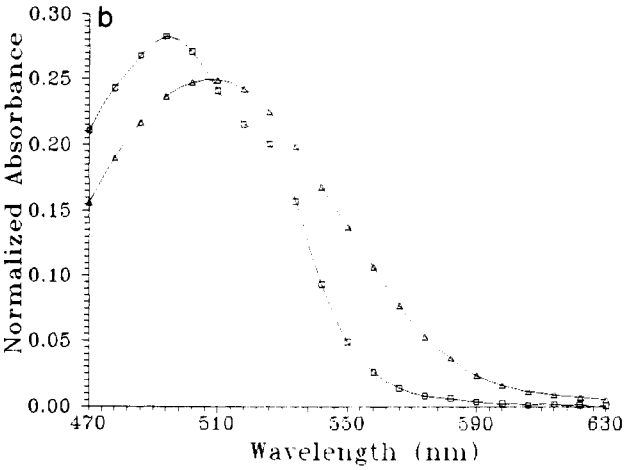

Figure 9. Solution bands for the spectra of the Co–PAR (a) and Ni–PAR complexes (b) obtained by processing the data in Figure 8; (△) lower limit; (□) upper limit.

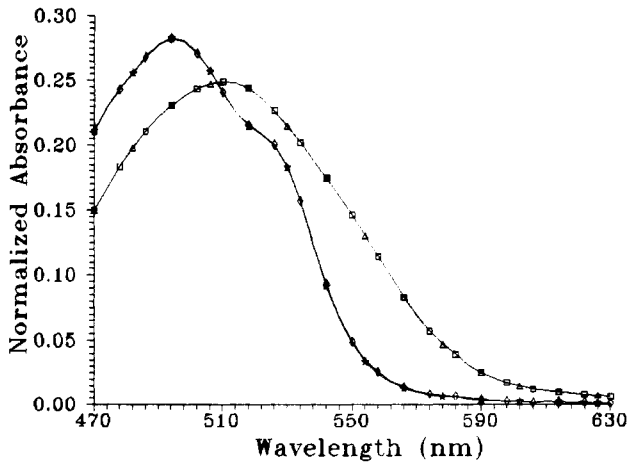

Figure 10. Real and reconstructed spectra obtained by processing the data in Figure 8: (△) Co, real; (□) Co, reconstructed; (☆) Ni, real; (◇) Ni, reconstructed.

interference), the whole system could be resolved by determining the corresponding ϕ angle for Co yielding the estimation that best fitted the known spectrum. Figure 10 shows the real spectra and those estimated according to the previous reasoning.

Finally, Figure 11 shows the overall and individual kinetics of the process, either simulated or reconstructed by factor

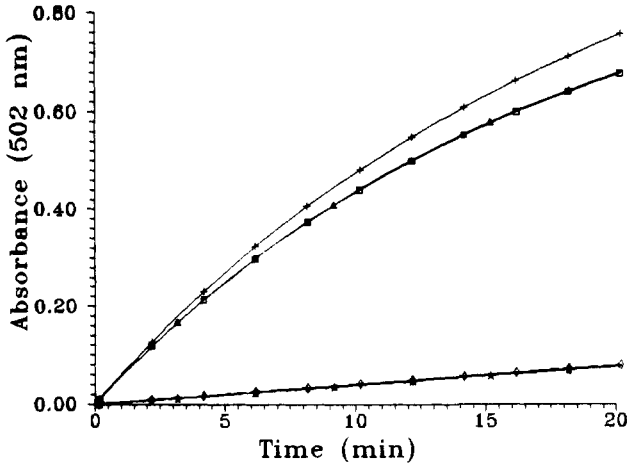

Figure 11. Simulated and reconstructed kinetic curves obtained from the data in Figure 8: (△) Co, simulated; (□) Co, reconstructed; (☆) Ni, simulated; (◇) Ni, reconstructed; (+) simulated overall kinetic curve.

analysis of the available data. Relatively larger deviations for the Ni–PAR complex are only obtained when the Ni concentration is much lower than that of Co, basically as a result of the smaller rate constant of the Ni–PAR complex compared to the Co–PAR complex and hence the smaller contribution of the former to the overall signal.

CONCLUSIONS

The proposed method for the resolution of simultaneous kinetic processes based on data processing by factor analysis has similar advantages and pitfalls as those previously used by other authors to resolve chromatographic signals. Even though it has only been applied to absorbance signals—the most common by far—in this work, it should be equally usable with other types of signals.

Unlike earlier methods for the resolution of simultaneous kinetic processes, the proposed method allows each of the individual kinetics involved in the chemical process concerned to be reconstructed with the need for no prior knowledge of the spectra of the components or a difference between the rate constants. On the other hand, estimation errors are avoided as no parameter values need be estimated.

The results obtained by applying the different variants are satisfactory taking into account the great difficulty involved in processing kinetic data on the basis of no known spectra. As a result, the obtainment of the purest spectra of each component involved poses some problems that can be solved in most instances. This is crucial since the quality of the reconstructed individual kinetics will logically be dictated by that achieved from each spectrum.

As a rule, the model for simultaneous kinetics of formation and disappearance provides the best results. Also, with kinetics evolving in the same direction, formation kinetics provide better results than do disappearance kinetics.

The chief limitations of the proposed method are the number of components that can be resolved (more than two call for rather a complex mathematical treatment) and the inherent constraints to the procedure, which preclude proper resolution in the following—fortunately rare—instances: (a) when the spectra of the two components are fully overlapped; (b) in the kinetic models for simultaneous formation or disappearance (types II and III) when the rate constants are identical; and (c) in the previous models when the spectrum of one of the components envelops that of the other throughout the process.

ACKNOWLEDGMENT

The authors wish to express their gratitude to the DGICyT (Spanish Council for Research in Science and Technology) for financial support awarded through Project PB 90-0359.

RECEIVED for review August 4, 1992. Accepted November 25, 1992.